JOURNAL OF THERMOPHYSICS AND HEAT TRANSFER
Vol. 11, No. 2, April–June 1997

Magnetic Damping of Buoyant Convection During Semiconductor Crystal Growth with *g*-Jitters

Nancy Ma* and John S. Walker†
University of Illinois at Urbana–Champaign, Urbana, Illinois 61801

In the Bridgman process, a single crystal is grown by the directional solidification of an initially molten semiconductor (melt) contained in a cylindrical ampoule. A crystal-growth experiment in an Earth-orbiting vehicle is subjected to unsteady residual accelerations (*g*-jitters), which drive an undesirable oscillatory buoyant convection in the melt. Since many molten semiconductors are excellent electrical conductors, the magnitude of the buoyant convection is dramatically reduced by applying a magnetic field during crystal growth. We treat the buoyant convection driven by periodic *g*-jitters whose direction is parallel to the axis of the ampoule. There is a nonuniform magnetic field that is axisymmetric around the ampoule axis. We compare the magnitudes and characteristics of the buoyant convections for various nonuniform magnetic fields to those for a uniform axial magnetic field.

Introduction

THE electrical properties of semiconductor crystals depend on the concentrations of certain other elements (dopants) in the crystal. For segregation coefficients of less than one, dopant is rejected back into the melt during crystallization. If the rejected dopant remains trapped and radially uniform inside a mass-diffusion boundary layer adjacent to the crystal-melt interface, then the dopant concentration over most of the crystal length is uniform and equal to the original concentration in the melt. This desirable diffusion controlled condition is difficult to achieve. During terrestrial crystal growth, the buoyancy-driven convection transports rejected dopant from the mass-diffusion boundary layer to the bulk of the melt and produces temporal oscillations in the concentration inside the layer. In the final crystal, the dopant concentration varies over both the length and radius of the crystal (axial and radial macrosegregation), and there are spatial oscillations in the dopant concentration on a micrometer scale (microsegregation or striations). In an Earth-orbiting vehicle, *g*-jitters drive an oscillatory buoyant convection that also produces striations and provides mixing between the mass-diffusion boundary layer and the bulk of the melt, again leading to macrosegregation.

To achieve the ideal crystals from diffusion-controlled growth, NASA has begun to design a magnetic damping furnace for space flights in 1999 and beyond.[1] Semiconductor crystals will be grown by the Bridgman process with an externally applied magnetic field that will have a magnetic flux density of $B_0 = 0.2$ T. Hjellming and Walker[2] gave the characteristic velocity for magnetically damped buoyant convection

$$U_c = \frac{\rho\beta(\Delta T)\alpha g_0}{\sigma B_0^2} \tag{1}$$

where ρ, β, and σ are the density, volumetric expansion coefficient, and electrical conductivity of the melt, respectively; whereas (ΔT) is the characteristic temperature difference in the melt, αg_0 is the characteristic magnitude of the *g*-jitters, and $g_0 = 9.81$ m/s^2. Typical *g*-jitters consist of continuous and chaotic accelerations with $\alpha = 10^{-4}$–10^{-3}, caused by crew movements, machinery, etc., plus isolated spikes with α as large as 10^{-2}, as a result of thruster firing, equipment deployment, etc.[3] Equation (1) shows that the magnitude of the oscillatory buoyant convection decreases as B_0^{-2} as the magnetic flux density is increased. For the properties of molten silicon and for NASA's tentative design with $B_0 = 0.2$ T, $U_c = 0.7$ μm/s for $\alpha = 10^{-3}$. This will be our typical case for estimating parameter values.

In a previous paper,[4] we presented numerical solutions for the *g*-jitter-driven buoyant convection with a uniform axial magnetic field, i.e., parallel to the axis of the ampoule. One advantage of a magnetic field is that it can be tailored by changing the relative position of the solenoid to achieve a wide variety of nonuniform fields. For the terrestrial Czochralski process with the melt in an open crucible, crystals grown in certain nonuniform, axisymmetric magnetic fields have more uniform distributions of dopants and of oxygen compared to crystals grown in a uniform magnetic field.[5]

Our objective is to investigate whether any nonuniform, axisymmetric magnetic field is more effective in the suppression of *g*-jitter-driven buoyant convection in the Bridgman process than a uniform axial magnetic field would be. To compare buoyant convections for a uniform field and for a nonuniform field, or for two different nonuniform fields, we use the same rms magnetic flux density for every case, with the mean taken over the volume of the melt. With this rms value for B_0, the characteristic velocity defined by Eq. (1) is the same for every magnetic field configuration.

Problem Formulation

The electric currents in the melt produce an induced magnetic field that is superimposed on the applied magnetic field produced by the permanent magnet or solenoid. The characteristic ratio of the induced to applied magnetic field strengths is the magnetic Reynolds number, $R_m = \mu_p \sigma U_c R$, where μ_p is the magnetic permeability and R is the inside radius of the ampoule. For our typical case, $R_m = 8 \times 10^{-9}$, so that the induced magnetic field is negligible. An axisymmetric magnetic field has only radial and axial components, B_r and B_z, which depend only on the dimensionless cylindrical coordinates r and z, with the z axis along the centerline of the am-

Presented as Paper 96-0252 at the AIAA 34th Aerospace Sciences Meeting, Jan. 15–19, 1996, Reno, NV; received June 27, 1996; revision received Sept. 20, 1996; accepted for publication Sept. 20, 1996.

*Research Assistant, Department of Mechanical and Industrial Engineering.

†Professor, Department of Mechanical and Industrial Engineering.

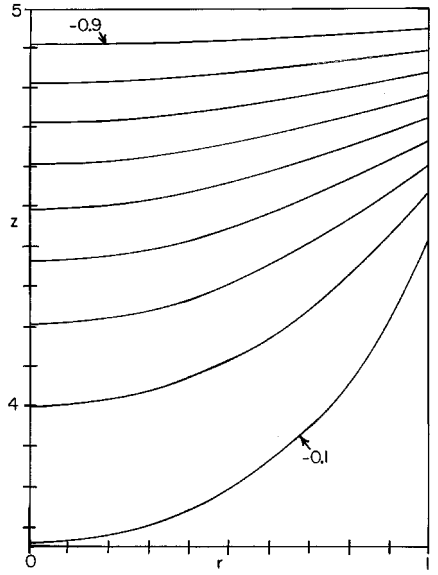

Fig. 1 Isotherms for the deviation from the hottest temperature in the melt, normalized by the overheat temperature: $T = -1$ at the crystal-melt interface at $z = 5$ and $T = 0$ for $0 < z < 3.65$.

poule and with the origin at the center of the hotter end of the ampoule. The magnetic field is governed by

$$\frac{\partial B_r}{\partial r} + \frac{B_r}{r} + \frac{\partial B_z}{\partial z} = 0 \tag{2a}$$

$$\frac{\partial B_r}{\partial z} = \frac{\partial B_z}{\partial r} \tag{2b}$$

with suitable boundary conditions at the surfaces of the solenoid coils. With B_r and B_z normalized by B_0

$$\int_0^b \int_0^1 (B_r^2 + B_z^2) r \, dr \, dz = 0.5b \tag{3}$$

where b is the instantaneous axial distance between the hotter end of the ampoule and the crystal-melt interface, normalized by R.

In the heat equation, Joulean heating and viscous dissipation are negligible.[6] The characteristic ratio of convective heat transfer to thermal conduction is the Péclét number, $Pe = \rho c_h U_c R/k$, where c_h and k are the specific heat and thermal conductivity of the melt, respectively. For our typical case, $Pe = 3 \times 10^{-4}$, so that $\nabla^2 T = 0$, where T is the deviation of the dimensional temperature from the hottest melt temperature, normalized by (ΔT), which we choose as the difference between the hottest temperature and the solidification temperature, i.e., the melt's overheat temperature. The isotherms for $b = 5$ and for a typical Bridgman heater are presented in Fig. 1, where $T = -1$ at the crystal-melt interface at $z = 5$ and $T = 0$ for $0 < z < 3.65$.

In the Navier–Stokes equation, the characteristic ratio of the electromagnetic body force term, $\boldsymbol{j}^* \times \boldsymbol{B}^*$, to the nonlinear inertial term, $\rho(\boldsymbol{v}^* \cdot \nabla)\boldsymbol{v}^*$, is the interaction parameter, $N = \sigma B_0^2 R/\rho U_c$, where an asterisk denotes a dimensional variable, $\boldsymbol{j}^*$ is the electric current density, $\boldsymbol{B}^*$ is the magnetic flux vector, and $\boldsymbol{v}^*$ is the melt velocity. For our typical case, $N = 2 \times 10^5$, so that the nonlinear inertial term is negligible. With these assumptions, the boundary-value problem governing the oscillatory buoyant convection driven by the fluctuating g-jitters is linear. The direction of the g-jitter vector varies with time. With linearity, we can obtain the solution for any directional history with the time-dependent superposition of solutions for two unidirectional g-jitters: one axial and one transverse. Here we only treat the axial g-jitter solution. In addition, the response to a continuous and chaotic g-jitter history can be obtained by a Fourier-transform superposition of solutions for sinusoidal histories for all frequencies. Therefore, we only treat axial g-jitters whose dimensionless magnitude is $\cos(\omega t)$, where t is time normalized by a characteristic magnetic damping time, $\rho/\sigma B_0^2 = 0.05$ s, and ω is the dimensionless circular frequency.

In the Navier–Stokes equation, the characteristic ratio of the electromagnetic (EM) body force term to the viscous term is Ha^2, where $Ha = B_0 R(\sigma/\mu)^{1/2}$ is the Hartmann number, and μ is the melt's viscosity. For our typical case, $Ha = 61$. For $Ha \gg 1$ and $\omega \neq 0$, the melt can be subdivided into an inviscid core and boundary layers adjacent to the ampoule surfaces and to the crystal-melt interface. All three boundary layers have an $\mathcal{O}(Ha^{-1})$ dimensionless thickness and have simple exponential structures that satisfy the no-slip condition at the boundary and match any tangential core velocity.[4] With $Ha = 61$, the boundary layers are thin and play no significant role in the flow, so that we ignore them and treat the inviscid core flow.

For a steady, axisymmetric temperature and for periodic axial g-jitters, the periodic buoyant convection is axisymmetric. The dimensionless governing equations are

$$\frac{\partial v_r}{\partial t} = -\frac{\partial p}{\partial r} + B_z j_\theta \tag{4a}$$

$$\frac{\partial v_z}{\partial t} = -\frac{\partial p}{\partial z} - B_r j_\theta + T\cos(\omega t) \tag{4b}$$

$$j_\theta = B_r v_z - B_z v_r \tag{4c}$$

$$\frac{\partial v_r}{\partial r} + \frac{v_r}{r} + \frac{\partial v_z}{\partial z} = 0 \tag{4d}$$

Here, v_r and v_z are the radial and axial velocity components, respectively, normalized by U_c; j_θ is the azimuthal electric current density, normalized by $\sigma U_c B_0$; p is the pressure deviation from the hydrostatic pressure caused by g-jitters with a uniform density, normalized by $\sigma U_c B_0^2 R$; and B_r, B_z, and T are known functions of r and z. Equations (4a) and (4b) are the radial and axial components of the Navier–Stokes equation without the nonlinear inertia terms and the viscous terms, Eq. (4c) is the azimuthal component of Ohm's law with zero electric field because of axisymmetry, and Eq. (4d) is the continuity equation. We introduce Eq. (4c) into Eqs. (4a) and (4b), we cross-differentiate to eliminate p, and we introduce the stream function ψ, where

$$v_r = \frac{1}{r}\frac{\partial \psi}{\partial z} \tag{5a}$$

$$v_z = -\frac{1}{r}\frac{\partial \psi}{\partial r} \tag{5b}$$

The result is a single equation governing $\psi(r, z, t)$, with the boundary conditions

$$\psi = 0 \quad \text{at} \quad r = 1, \quad z = 0 \quad \text{and} \quad z = b \tag{6}$$

Since the equation governing ψ is linear, ψ has only one Fourier component in time, so that $\psi = \psi_c(r, z)\cos(\omega t) + \psi_s(r, z)\sin(\omega t)$. Here, ψ_c is the buoyant convection that is in phase with the g-jitters, and ψ_s is the convection that follows the g-jitters by a quarter period. We solve the two coupled differential equations governing ψ_c and ψ_s and the conditions [Eq. (6)] using a Chebyshev spectral collocation method.

Results

For all of the results presented here, we used $b = 5$ and the $T(r, z)$ whose isotherms are presented in Fig. 1. We chose a simple nonuniform, axisymmetric magnetic field with

$$B_r = Cr \tag{7a}$$

$$B_z = 2C(ab - z) \tag{7b}$$

which satisfy Eqs. (2). Equation (3) gives $C = [0.5 + 4b^2(a^2 - a + 1/3)]^{-1/2}$. This magnetic field is a cusp field caused by two axially opposed solenoids where the axial fields caused by the two solenoids cancel at $z = ab$, so that the field is purely radial in this plane. We consider three cases. Our base case is a uniform axial magnetic field with $B_r = 0$ and $B_z = 1$, corresponding to $a >> 1$. We use Eqs. (7) with $a = 10^6$ for this case. Our second case for $a = 1$ has a weak, purely radial magnetic field at the crystal-melt interface and has the strongest field at the hotter end of the ampoule. For $a = 1$, B_z decreases linearly from 1.719 at $z = 0$ to zero at $z = 5$, whereas B_r increases linearly from zero at $r = 0$ to 0.1719 at $r = 1$. Our third case with $a = 0$ is the axial inverse of the field for $a = 1$, so that the magnetic field is weak and purely radial at the hotter end of the ampoule and is strongest at the crystal-melt interface, i.e., B_z varies linearly from zero at $z = 0$ to -1.719 at $z = 5$. For every value of ω and with $a = 10^6$, our results agree to six significant figures with our previous results for a uniform axial magnetic field.[4] These previous results were obtained with a different formulation involving an integration function that cannot be used here because B_r and B_z are spatially variable coefficients in Eqs. (4).

When ω is small, the time derivatives on the left-hand sides of Eqs. (4a) and (4b) are small, and only the EM body force opposes the buoyant convection. As ω is increased, inertial opposition to the convection is added to the EM force, so that the magnitude of the buoyant convection decreases. At very small values of ω, the convection is nearly in phase with the g-jitters, i.e., ψ_c is larger than ψ_s. As ω is increased, the convection shifts toward a quarter-period lag after the g-jitters. For $\omega > 1$, ψ_c and ψ_s vary as ω^{-2} and ω^{-1}, respectively.[4] The effects of tailoring the magnetic field are larger for small values of ω, when the EM force dominates, than for large values of ω, when inertial effects dominate.

The streamlines of ψ_c and ψ_s for $\omega = 0.1$ and $a = 1$ are presented in Fig. 2. For every case, the convection is concentrated near the crystal-melt interface, and more than half of the melt near the hotter end is essentially stagnant. Therefore, the principal effect of tailoring the magnetic field is to increase or decrease the local magnetic field strength in the region of the convection. With $a = 1$, the field is weak near the crystal-melt interface, so that EM opposition to the buoyant convection is less than that for a uniform axial magnetic field. Reducing the local EM opposition allows the convection to increase and shifts the phase closer to a quarter-period lag because inertial effects play a larger relative role. As a is changed from 10^6 to 1 for $\omega = 0.1$, the magnitude of the buoyant convection increases by 93%, and the ratio of the phase lag to a quarter period increases from 0.53 to 0.86. With $a = 0$, the magnetic field is strongest near the crystal-melt interface, so that the local EM opposition is larger than that for a uniform axial magnetic field. As a is changed from 10^6 to 0 for $\omega = 0.1$, the magnitude of the buoyant convection decreases by 35%, and the ratio of the phase lag to a quarter period decreases to 0.41.

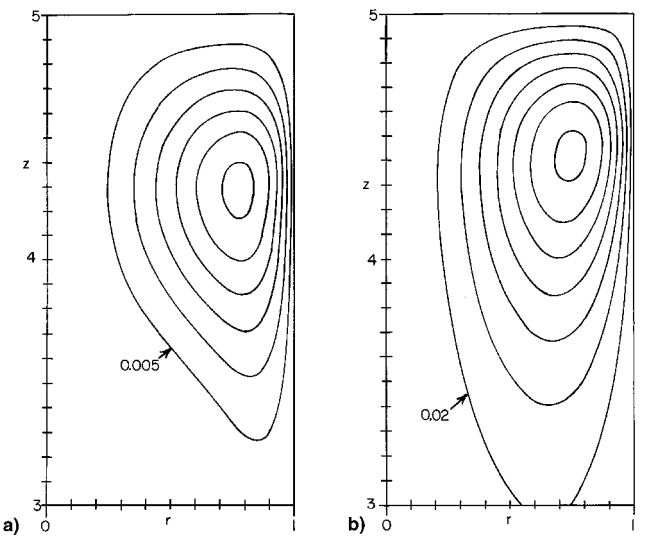

Fig. 2 Streamlines for $\omega = 0.1$ and $a = 1$: a) $\psi_c = 0.005n$ for $n = 1$–6 and b) $\psi_s = 0.02n$ for $n = 1$–7.

Khine and Walker[7] found that tailoring the nonuniform, axisymmetric magnetic field dramatically changed the streamline patterns for buoyant convection in the Czochralski process. Therefore, we were surprised to find very small differences between the streamline patterns for $a = 0$, 1, and 10^6 and for any value of ω. For example, as a is changed from 1 to 0 for $\omega = 0.1$, the location of the maximum value of ψ_c shifts from $z = 4.27$ in Fig. 2a to $z = 4.15$.

As the value of ω is increased, the effects of tailoring the magnetic field decrease. For $\omega = 1$, changing a from 10^6 to 1 or 0 increases or decreases the magnitude of the buoyant convection by 3.3 or 9.6%, respectively. For $\omega = 1$, all of the phase lags are close to a quarter period.

Conclusions

We have considered the effects of tailoring a nonuniform, axisymmetric magnetic field on the buoyant convection driven by periodic, axial g-jitters in the ampoule of a Bridgman process. Relative to a uniform, axial magnetic field, the effect of tailoring the field is to increase or decrease the field strength near the crystal-melt interface where the convection is concentrated. For a low frequency, a tailored magnetic field with the largest field strength near the crystal-melt interface led to 35% less buoyant convection than that for a uniform axial field. However, this comparison assumes that the rms magnetic flux density B_0 is the same for the uniform and nonuniform magnetic fields. A solenoid produces a relatively strong and nearly uniform magnetic field near its center and a much weaker nonuniform, axisymmetric magnetic field just outside either end. Therefore, our actual choice is between a nearly uniform field with a larger flux density and a nonuniform field with a smaller rms flux density. We should make the comparison for a given solenoid, not for the same rms flux density. For both nonuniform fields considered here, the axial magnetic field is $1.72B_0$ at one end of the melt, so that the uniform field in the center of the solenoid must be at least this strong. If we compare the nonuniform field with the strongest field at the crystal-melt interface and with a rms magnetic flux density of B_0 to a uniform field with a flux density of $1.72B_0$, we find that the magnitude of the buoyant convection for the uniform field is 64% less than that for the nonuniform field because the characteristic velocity varies as the inverse square of the magnetic flux density. We conclude that one wants to place the melt in the region of largest magnetic flux density available with a given solenoid or magnet, and that will generally be the most uniform part of the field.

Acknowledgments

This research was supported by NASA Cooperative Research Agreement NCC8-90 and by the National Science Foundation under Grant CTS 94-19484. The calculations were performed on the Convex C3880 supercomputer at the National Center for Supercomputer Applications at the University of Illinois at Urbana–Champaign.

References

[1]Anon., "Microgravity Materials Science: Research and Flight Experiment Opportunities," NASA Research Announcement, 94-OLMSA-06, Dec. 1994.

[2]Hjellming, L. N., and Walker, J. S., "Melt Motion in a Czochralski Crystal Puller with an Axial Magnetic Field: Motion Due to Buoyancy and Thermocapillarity," *Journal of Fluid Mechanics*, Vol. 182, 1987, pp. 335–368.

[3]Hamacher, H., Fitton, B., and Kingdon, J., "The Environment of Earth Orbiting Systems," *Fluid Sciences and Materials Science in Space*, edited by H. U. Walter, Springer–Verlag, Berlin, 1987, pp. 1–50.

[4]Ma, N., and Walker, J. S., "Magnetic Damping of Buoyant Convection During Semiconductor Crystal Growth in Microgravity: Continuous Random *g*-Jitters," *Physics of Fluids*, Vol. 8, No. 4, 1996, pp. 944–953.

[5]Series, R. W., and Hurle, D. T. J., "The Use of Magnetic Fields in Semiconductor Crystal Growth," *Journal of Crystal Growth*, Vol. 113, 1991, pp. 305–328.

[6]Langlois, W. E., and Lee, K. J., "Czochralski Crystal Growth with an Axial Magnetic Field: Effects of Joulean Heating," *Journal of Crystal Growth*, Vol. 62, 1983, pp. 481–486.

[7]Khine, Y. Y., and Walker, J. S., "Buoyant Convection During Czochralski Silicon Growth with a Strong, Non-Uniform, Axisymmetric Magnetic Field," *Journal of Crystal Growth*, Vol. 147, 1995, pp. 313–319.